Available online at www.sciencedirect.com
SCIENCE DIRECT®
Analytical Biochemistry 340 (2005) 259–271
ANALYTICAL BIOCHEMISTRY
www.elsevier.com/locate/yabio

A high-throughput fluorescence–anisotropy screen that identifies small molecule inhibitors of the DNA binding of B-ZIP transcription factors

Vikas Rishi [a], Timothy Potter [b], Julie Laudeman [b], Russel Reinhart [b], Thomas Silvers [b], Michael Selby [b], Timothy Stevenson [b], Paula Krosky [b], Andrew G. Stephen [b], Asha Acharya [a], Jon Moll [a], Won Jun Oh [a], Dominic Scudiero [b], Robert H. Shoemaker [c], Charles Vinson [a,*]

[a] *Laboratory of Metabolism, National Cancer Institute, National Institutes of Health, Bethesda, MD 20892, USA*
[b] *Science Applications International Corporation (SAIC), Frederick, MD 21702, USA*
[c] *Developmental Therapeutics Program, National Cancer Institute, Frederick, MD 21702, USA*

Received 5 November 2004
Available online 16 March 2005

Abstract

We have developed a high-throughput fluorescence anisotropy screen, using a 384-well format, to identify small molecules that disrupt the DNA binding of B-ZIP proteins. Binding of a B-ZIP dimer to fluorescently labeled DNA can be monitored by fluorescence anisotropy. We screened the National Cancer Institute diversity set of 1990 compounds to identify small molecules that disrupt the B-ZIP|DNA complex of CREB, C/EBPβ, VBP, and AP-1 (FOS|JUND) bound to their cognate DNA sequence. We identified 21 compounds that inhibited the DNA binding of at least one B-ZIP protein, and 12 representative compounds were grouped depending on whether they displaced ethidium bromide from DNA. Of the 6 compounds that did not displace ethidium bromide, 2 also inhibited B-ZIP binding to DNA in a secondary electrophoretic mobility shift assay screen with some specificity. Thermal stability monitored by circular dichroism spectroscopy demonstrated that both compounds bound the basic region of the B-ZIP motif. NSC13778 preferentially binds C/EBPα 1000-fold better than it binds C/EBPβ. Chimeric proteins combining C/EBPα and C/EBPβ mapped the binding of NSC13778 to three amino acids immediately N terminal of the leucine zipper of C/EBPα. These experiments suggest that the DNA binding of B-ZIP transcription factors is a potential target for clinical intervention.
Published by Elsevier Inc.

Keywords: High-throughput screen; B-ZIP protein; Fluorescence anisotropy/fluorescence polarization; Small molecules; CREB; VBP; C/EBP; AP-1

The identification of small molecules that disrupt the function of specific cellular proteins is a powerful method to develop new pharmacological agents. Currently, certain classes of proteins have a rich collection of small molecules that disrupt their function, whereas other classes of proteins have no known small molecule inhibitors. For example, although several compounds that disrupt enzymatic activity have been identified, the search for small molecules that disrupt protein–protein interactions has proved to be more difficult. A recent report of the inhibition of p53 binding to MDM2 demonstrates the potential for small molecules to disrupt protein–protein interfaces [1].

The B-ZIP class of transcription factors are a group of 63 genes in the human genome [2] that mediate a variety of signaling pathways by binding to DNA as

* Corresponding author. Fax: +1 301 496 8419.
E-mail address: vinsonc@dc37a.nci.nih.gov (C. Vinson).

0003-2697/$ - see front matter. Published by Elsevier Inc.
doi:10.1016/j.ab.2005.02.012

homo- or heterodimers and regulating gene expression. The AP-1 (activator protein-1)[1] [3,4], CREB (cyclic AMP response element binding protein) [5,6], and C/EBP (CCAAT/enhancer binding protein) families [7] of B-ZIP proteins have been identified as potential molecular targets for a variety of human pathologies, including cancer and diabetes. Unfortunately, there are no known small molecules that can disrupt the DNA binding of individual members of the B-ZIP family of 63 genes. This has hindered our ability to ascertain whether these proteins are potential targets for clinical intervention.

We have developed a high-throughput screen to identify small molecules that disrupt the DNA binding of the B-ZIP proteins. Fluorescence anisotropy/fluorescence polarization is a spectroscopic technique that measures the tumbling rate of a sample. It uses polarized light to excite a fluorophore and measures the polarization characteristics of the fluoresced light (for a review, see [8]). If the sample tumbles slowly relative to the fluorescence lifetime, the fluoresced light retains some polarization. However, if the sample tumbles rapidly, the fluoresced light loses its polarization. Thus, the degree of anisotropy (polarization) of the fluoresced light emitted from a sample gives a measure of the rotational speed of the sample. This technique can be used to monitor the binding of two molecules to each other. The observed fluorescence is a weighted average of the bound or unbound states of the excited fluorophore and can be presented as fluorescence polarization or fluorescence anisotropy, two mathematical descriptions that can easily be converted to one another. Fluorescence polarization assays have been developed for a variety of biochemical interactions, including actin binding proteins [9], tyrosine kinases [10], protease activity [11], G protein-coupled receptors [12], and signal transducer and activator of transcription (STAT)–receptor interactions [13]. We show here that this type of assay can be adopted for identifying small molecules that disrupt B-ZIP protein binding to DNA. To the best of our knowledge, this is the first high-throughput screen that uses fluorescence polarization to study the ability of small molecules to disrupt the DNA binding of the B-ZIP class of transcription factors.

Typically, to monitor a change in fluorescence anisotropy caused by a binding reaction, the fluorescently labeled protein is smaller than the unlabeled protein. However, a B-ZIP dimer binding to a similar-sized labeled DNA oligonucleotide caused a dramatic slowing in tumbling, presumably due to the T-shaped structure of the B-ZIP|DNA complex.

We have developed a high-throughput fluorescence anisotropy screen in 384-well plates to identify small molecules that disrupt the DNA binding of B-ZIP proteins to DNA. Our initial screen used the National Cancer Institute (NCI) diversity set of 1990 compounds, a group of compounds that represent a wide variety of chemical structures [14–16]. We ran the screen in parallel, using four B-ZIP proteins binding to their cognate DNA sequence, and identified 21 compounds that disrupted the B-ZIP|DNA complex. We used three secondary screens to reject compounds that either bound to DNA or showed no selectivity in B-ZIP binding, ethidium bromide displacement assay, electrophoretic mobility shift assay (EMSA), and circular dichroism (CD) spectroscopy. We identified 2 compounds that bind to the basic region of the B-ZIP dimer and disrupt DNA binding.

Materials and methods

Proteins

The majority of the B-ZIP domain proteins used in this study have been described elsewhere: VBP (vitellogenin gene binding protein) [17], C/EBP [18], CREB [19], c-FOS [20], and SREBP-1 (sterol regulatory element binding protein) [21]. All proteins used in this study have 13 amino acid Phi 10 epitopes at their N terminal. The c-JUND protein has the following amino acid sequence: SPIDMESQERIKAERKRMRNRIAA SKCRKRKLERIARLEEKVKTLKAQNSELASTAN MLREQVAQLKQKVMNHVNSGCQLMLTQQLQT F. The sequence of C/EBPβ is KAKKTVDKHSDEY KIRRERNNIAVRKSRDKAKMRNLETQHKVLET AENERLQKKEVQLSRELSTLRNLFKQLPEPLLAS AGHC. For PCR amplifications, the following overlapping primers were used:

C/EBPβ(α): 5′-CAGCGCAACGTGGAGACGCA GCAGAAGGTCCTG-3′ and 5′-GTTGCGCTGC TTGGCCTTGTC-3
C/EBPα(β): 5′-GTGCTGCGTCTCCAGGTTGCG CATTTTGGCTTTATC-3′ and 5′-ATGCGCAAC CTGGAGACGCAGCACAAGGTGTTGGAG

PCR-amplified DNAs were cloned as *Bam*HI–*Hin*dIII insert in pT5 plasmid. Proteins were expressed in *Escherichia coli* BL-21 Lys(E) and purified as described previously [18]. For fluorescence anisotropy experiments, the sequences of the four 28-bp-long double-stranded DNAs were as follows:

[1] *Abbreviations used:* AP-1, activator protein-1; CREB, cyclic AMP response element binding protein; C/EBP, CCAAT/enhancer binding protein; STAT, signal transducer and activator of transcription; NCI, National Cancer Institute; EMSA, electrophoretic mobility shift assay; CD, circular dichroism; VBP, vitellogenin gene binding protein; SREBP-1, sterol regulatory element binding protein; SAIC, Science Applications International Corporation; DTT, dithiothreitol; DMSO, dimethyl sulfoxide.

CREB: 5′-F-GTCAGTCAGATGACGTCATATCG GTCAG-3′
FOS|JUND: 5′-F-GTCAGTCAGAATGACTCAT ATCGGTCAG-3′
VBP: 5′-F-GTCAGTCAGATTACGTAATATCGG TCAG-3′
C/EBP: 5′-F-GTCAGTCAGATTGCGCAATATC GGTCAG-3′

In these sequences, F is a fluorescein molecule attached to 5′ end of both strands of DNA. All DNAs were ordered from Sigma–Genosys and were HPLC purified.

High-throughput screen

Fluorescein-labeled DNA containing a consensus-binding site for each B-ZIP protein was added at 5 nM to a black 384-well polypropylene plate with a Biomek 2000 automated pipetting instrument. The corresponding B-ZIP protein was added at 300 nM for FOS|JUND, 400 nM for CREB, and 1000 nM for both C/EBPβ and VBP by the Biomek 2000. The test compounds were diluted to the required concentrations and transferred from the 96-well storage plates to the test plate by the Biomek 2000. After incubation for 60 min at room temperature, fluorescence polarization was measured on a Tecan Ultra plate reader with excitation at 485 nm and emission at 535 nm. Incubation longer than this does not change the fluorescent signals; thus, equilibrium is assumed to be reached in 1 h. Changes in fluorescent (anisotropy/polarization) values of fluorescein-labeled DNA were used to study binding events in the presence of small molecules. The resulting polarization data were used to calculate percentage control for each test compound and protein.

Ethidium bromide displacement assay

This assay, essentially following the method described by Boger et al. [22], examines the capacity for a small molecule to displace ethidium bromide from a hairpin of DNA as evidenced by a loss of fluorescence. This indicates that the small molecule could interact with DNA. Three DNA hairpins were prepared by the Molecular Technology Laboratory, Science Applications International Corporation (SAIC)–Frederick, and NCI–Frederick with the following sequences:

CREB: TGACGTCAAAAAATGACGTCA
AT rich: TTAATTAAAAAAATTAATTAA
GC rich: GGCCGGCCAAAAAGGCCGGCC

Each of these hairpins was added to a separate test plate with the Biomek 2000 at a concentration of 2 μM. Ethidium bromide was added at a concentration of 1 μM. Test compounds were diluted on a 96-well plate and added to the test plate (final concentrations of 191 pM to 100 μM). The test plate was read for fluorescence on a Tecan Ultra plate reader with excitation at 530 nm and emission at 590 nm.

DNA binding assay

For EMSA, six protein samples (final concentration of 20 nM dimer/1 ng dimer)—CREB, VBP, FOS|JUND, C/EBPα, C/EBPβ, and SREBP-1—were mixed with the required concentrations of compounds at room temperature and then added to 20 μl of gel shift reaction buffer (25 mM Tris (pH 8.0), 50 mM KCl, 0.5 mM EDTA, 2.5 mM dithiothreitol (DTT), 1% bovine serum albumin, and 10% glycerol), incubated for 10 min, and then mixed with 7 pg ^{32}P-radiolabeled double-stranded oligonucleotides containing a single consensus binding site for proteins. (Sequences were the same as those used for fluorescence anisotropy experiments except that for EMSA they were not fluorescein labeled and for SREBP the following sequence containing underlined SRE site was used: 5′-GTCAGTCAGACACCCCACTATCGGT CAG-3′.) This reaction mixture was incubated at 37 °C for 30 min and then at room temperature for 20 min and was resolved on 7.5% native gel using 25 mM Tris–borate running buffer (pH 8.0) with 0.3 mM EDTA at 150 V potential (11 mA current) for 90 min.

Circular dichroism spectroscopy

Typically, all stock solutions of compounds were prepared in 100% dimethyl sulfoxide (DMSO), and initial dilutions were made in CD buffer (12.5 mM phosphate buffer (pH 7.4), 150 mM KCl, 0.25 mM EDTA, and 1 mM DTT) without KCl. CD spectra were recorded at 6 °C on a JASCO J-720 spectropolarimeter in a 5-mm quartz cuvette using a scanning rate of 100 nm/min with a 1-nm interval at the spectral bandwidth of 2 nm. Each spectrum was an average of 10 individual spectra. All protein samples were in CD buffer with 0.1% DMSO and were equilibrated with different concentrations of compound at room temperature for at least 2 h. For thermal denaturation studies in the presence and absence of compounds, protein samples were heated from 6 to 85/90 °C with a heating rate of 1 °C/min, and changes in ellipticity were recorded at 227 nm. Each thermal denaturation curve was analyzed for T_m (midpoint of thermal transition) and ΔH_m (enthalpy change at T_m), as described previously [21]. Values of T_m and ΔH_m with a predetermined ΔC_p (heat capacity change on dimer formation) value of -1.2 kcal mol^{-1} dimer^{-1} K^{-1} [23] were used to obtain ΔG_{Di} (Gibbs free energy change

on dimer formation) according to the Gibbs–Helmholtz equation.

Results

Fig. 1A presents the X-ray structure of a B-ZIP homodimer bound to DNA [24]. Fig. 1B presents the increase in fluorescence polarization after a 28-bp double-stranded DNA, labeled with fluorescein at the 5′ ends of both DNA strands, binds to a FOS|JUND heterodimer. This indicates a slowing of the tumbling rate of the DNA on protein binding. Normally, the binding between two entities of similar mass does not produce an easily observable change in fluorescent anisotropy. However, in the case of B-ZIP binding to double-stranded DNA (molecular weights of all B-ZIP proteins used in this study fall in the range of 18,000–23,000, and the molecular weight of 28-bp fluorescein-labeled double-stranded DNA is approximately 19,000), we suggest that the tumbling of the rod-like DNA is changed due to the T shape of the B-ZIP|DNA complex. To examine whether the slow tumbling rate of DNA could be reversed and thus useful as a high-throughput screen, we added A-FOS, a dominant negative protein that forms a stable A-FOS|JUND heterodimer and prevents JUND from binding to DNA [20]. The remaining FOS protein is unable to bind to DNA without its partner JUND. The addition of A-FOS causes the fluorescence polarization to decrease nearly back to the baseline DNA-only value, suggesting that A-FOS disrupts the complexes between DNA and FOS|JUND (Fig. 1B).

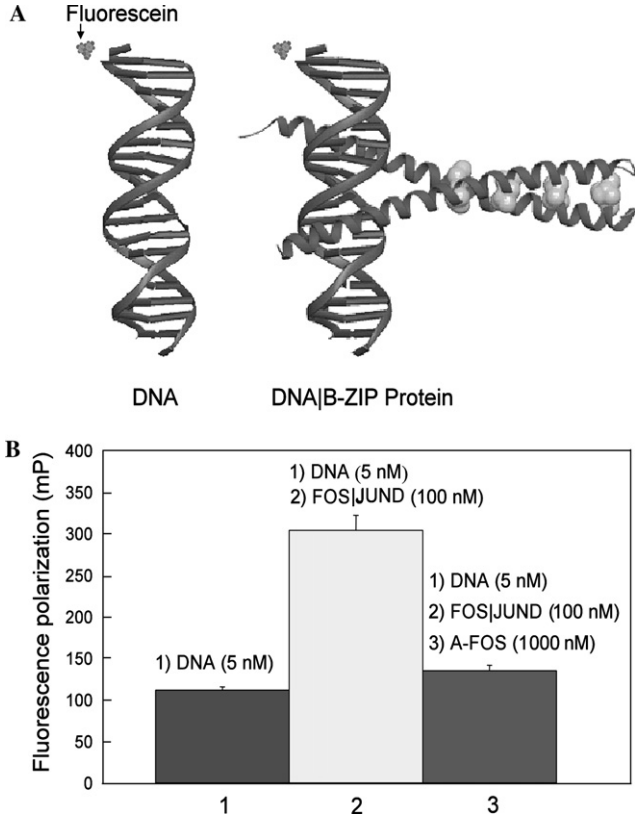

Fig. 1. (A) X-ray structure of 16-bp-long double-stranded DNA and a GCN4 B-ZIP domain bound to DNA [24]. The fluorescein molecule attached to the 5′ end of DNA is depicted to scale. The leucines in the "d" position are shown. (B) Fluorescence polarization data: (1) 5 nM of the 28-bp-long DNA containing the canonical AP-1 sequence labeled with fluorescein; (2) 5 nM of DNA bound by the 100-nM FOS|JUND heterodimer; (3) 5 nM DNA + 100 nM FOS|JUND heterodimer + 1000 nM A-FOS dominant negative protein.

Fig. 2 presents four titrations of increasing concentrations of the four B-ZIP proteins (CREB, FOS|JUND, VBP, and C/EBPβ) binding to 5 nM of a 28-bp fluorescein-labeled double-stranded DNA containing the consensus site for each B-ZIP dimer [23]. In all cases, there is an increase in fluorescence polarization. The C/EBPβ sample is saturated at 500 nM; however, the other three proteins show a dose-dependent increase in fluorescence polarization. The dissociation constant (K_D) calculated using this method is much larger than that observed using EMSA, with the latter being closer to 10 nM [23]. We suggest that somewhere in the fluorescence polarization assay, the B-ZIP protein is lost due to adsorption, a notorious problem with these proteins. B-ZIP proteins have an extended hydrophobic interface that has a tendency to stick to surfaces, leading to loss of material. A variety of attempts were made to lower the protein concentration needed to reach DNA binding saturation, including using siliconized plates and adding bovine serum albumin, but these attempts were unsuccessful.

High-throughput screen

Fig. 3 presents the outline for the high-throughput screen of four B-ZIP dimers, each binding a different fluorescently labeled double-stranded DNA, executed in parallel. Initially, 6.7 μl of B-ZIP dimer protein solution (protein stock solutions: FOS|JUND = 0.9 μM, CREB = 1.2 μM, C/EBPβ and VBP = 3 μM) in TKxtra buffer (pH 7.6, 50 mM Hepes, 150 mM NaCl, and 0.1% bovine γ-globulin) was dispensed. After 5 min, 6.7 μl of fluorescein-labeled DNA from 15 nM stock was added and incubated for an additional 5 min. Finally, 6.7 μl of compound (3- or 150-μM stock concentrations that were typically in 0.1% DMSO) was added. This mixture of B-ZIP protein, fluorescein-labeled DNA, and compound was further incubated for 60 min at room temperature to allow any potential rearrangement of B-ZIP and DNA to occur. Fluorescence polarization of the solution was measured on a Tecan Ultra fluorescence reader.

Fig. 4 presents typical data from the screen for all four B-ZIP proteins bound to DNA and treated with

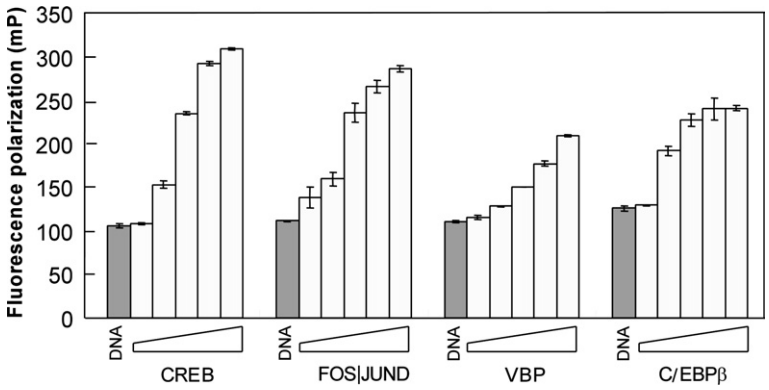

Fig. 2. DNA binding titration for four B-ZIP dimers (CREB, FOS|JUND, VBP, and C/EBPβ) binding to fluorescein-labeled 28-bp double-stranded DNA containing the consensus site for each B-ZIP dimer. Each DNA was added at 5 nM to a black 384-well polypropylene plate with a Biomek 2000 automated pipetting instrument. Each corresponding protein was added at five concentrations: 10, 100, 250, 500, and 1000 nM. After a 10-min incubation, fluorescence polarization was measured on a Tecan Ultra plate reader with excitation at 485 nm and emission at 535 nm.

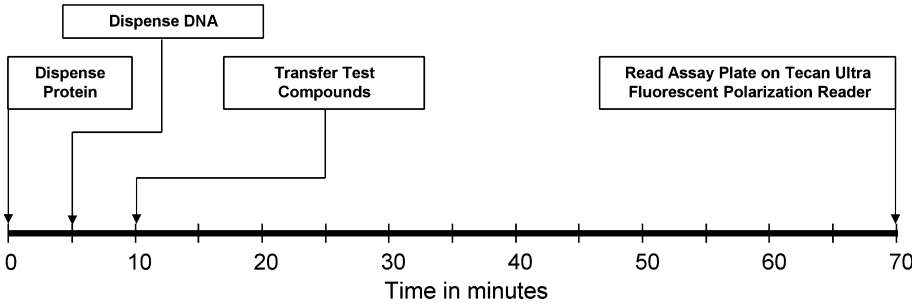

Fig. 3. Schematic of the timeline for the high-throughput binding fluorescence anisotropy DNA screening assay.

experimental compounds at two concentrations: 1 and 50 μM. At 1 μM (Fig. 4A), the fluorescence polarization shows little variation from sample to sample, often being within 80% of the control sample. One clear active compound is observed in this panel (NSC7223). At 50 μM (Fig. 4B), there were considerably more active compounds and more autofluorescent compounds. The fluorescence polarization reader optimizes the signal it receives from the fluorescent tag when measurements are taken, creating a functional range of polarization values. This optimization is based on the signal produced by fluorescein-labeled DNA. Some compounds generate a fluorescent signal above the range of polarization values. These compounds are designated autofluorescent and cannot be analyzed. Because of the high background fluorescence at 50 μM, we analyzed only the 1-μM data. Included in Fig. 4 is the Z' factor (a dimensionless screening window coefficient that depicts the assay range and data variation) calculated for the four proteins on this assay plate. All values are well over 0.5, indicative of a statistically significant assay [25].

Fig. 5 presents a summary of the fluorescence polarization change for fluorescein-labeled DNA bound by C/EBPβ when challenged with a 1-μM concentration of the 1990 compounds in the diversity set. The vast majority of compounds have little effect on fluorescence polarization. Of the 1990 compounds tested at a single concentration of 50 μM, 58 could not be evaluated due to autofluorescence and high backgrounds. Similarly, 2 compounds from the 1-μM actives could not be evaluated. In addition, 14 compounds were considered active in the screen because they decreased fluorescence polarization to less than 50% of control, returning the tumbling rate of the DNA to the faster mode observed when the DNA twirls along its long axis. Similar distributions are observed for the other three B-ZIP proteins.

Also, 39 compounds decreased fluorescence polarization to less than 50% of controls for at least one B-ZIP protein, and 21 were active when titrated in the four fluorescence anisotropy screens at 20 concentrations of each compound, ranging from 9.54×10^{-5} to 50 μM, a confirmation rate of 50%. Table 1 shows that most of the compounds that decreased fluorescence to less than 50% for multiple B-ZIP proteins were confirmed in multiple-dose titrations. Compounds affecting only one protein at 1 μM had only a 26% confirmation rate. Thus, the initial screening using multiple proteins yielded robust reproducible data. Table 2 presents the EC_{50} (compound concentration (in micromolars) at which fluorescence polarization value falls to 50% of the control) values for the 21 compounds that were active in this rescreen, an approximate 50% confirmation rate. These

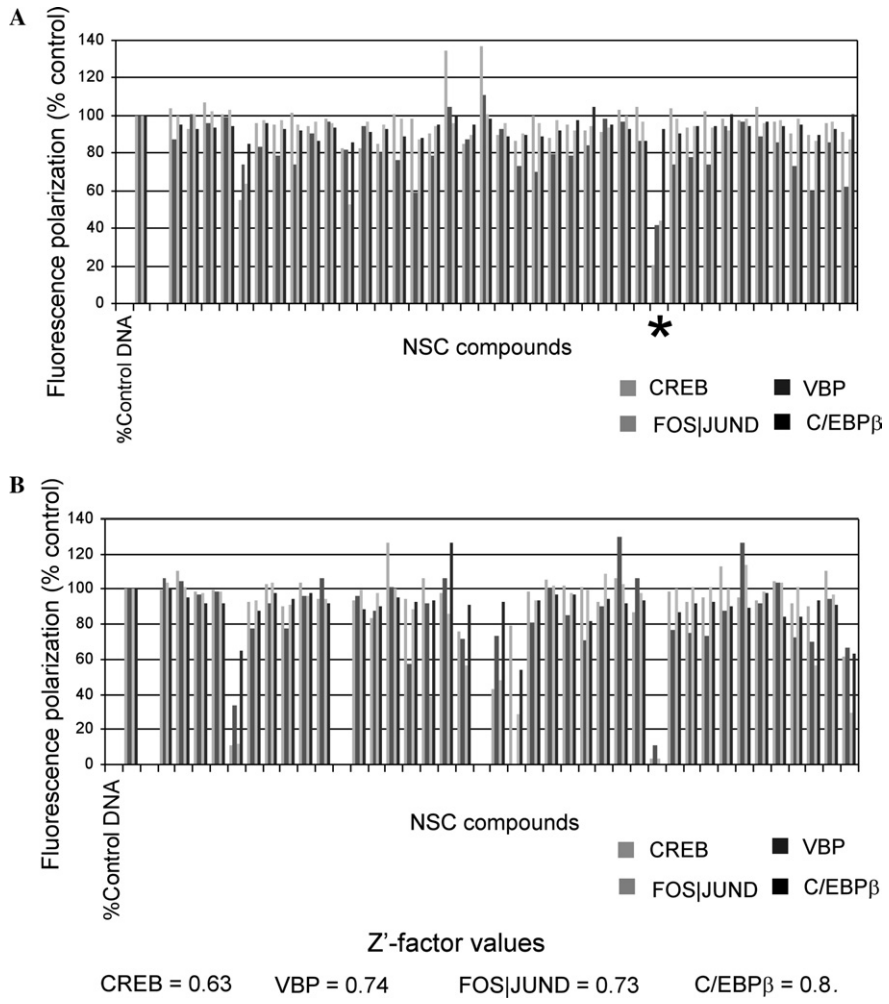

Fig. 4. Typical sample of the data from the four screens using the diversity set of compounds. Data for 1-μm (A) and 50-μm (B) concentrations are presented. Clear active compound NSC7223 is shown as an asterisk. The Z' factor statistical parameter was calculated according to Zhang et al. [25].

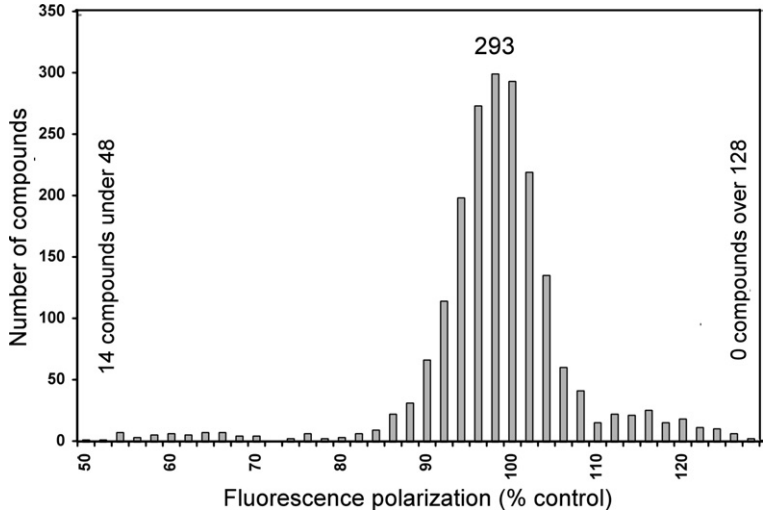

Fig. 5. Changes in fluorescence polarization after the addition of 1 μm compound for the 1990 compounds tested presented as a histogram for the C/EBPβ diversity set. Most compounds do not affect fluorescent polarization, and only 14 decrease it to less than 50% of control.

Table 1
Summary of confirmation testing of primary screen actives

Number of B-ZIP proteins where compounds were active	Number of active compounds at 1 μM	Number of actives on retesting	Percentage confirmation
4	3	3	100
3	8	8	100
2	5	4	80
1	23	6	26

Table 2
EC_{50} values (μM) of 21 actives from rescreen for four B-ZIP proteins

NSC number	EC_{50}			
	C/EBPβ	CREB	FOS|JUND	VBP
119911	24.7	1.6	0.1	10.4
119913	23.2	3.3	0.1	5.9
12155	2.5	0.6	—	—
13778	15.3	13.9	2.5	15.3
146443	3.2	23.0	—	16.1
172033	—	—	—	5.2
176327	4.7	—	0.8	4.3
210627	4.5	18.7	1.1	—
211736	—	—	3.1	—
270718	7.8	20.7	2.7	—
292213	—	—	7.4	—
293161	32.3	32.2	7.5	—
306698	—	—	—	1.4
306711	12.9	22.1	4.6	—
311152	5.5	—	3.4	—
328481	—	—	25.0	13.0
45576	24.1	11.9	—	—
50155	—	—	0.8	—
65828	34.2	28.0	8.9	—
223	3.7	3.5	2.1	0.7
73101	—	—	9.9	8.1

21 compounds were the ones that were active in more than one of the four primary screens.

Ethidium bromide displacement assay

The inhibition of B-ZIP binding to DNA could be caused by the organic compound binding to either the DNA or the protein. To help ascertain whether the compound is interacting with the DNA, 12 representative compounds identified as active in the titration analysis were used in an ethidium bromide displacement assay [22]. This assay assumes that if the compound binds to DNA, it will displace prebound ethidium bromide that can be measured by a decrease in fluorescence. Fig. 6 shows data for 2 compounds tested in both the fluorescence polarization and ethidium bromide displacement assays. NSC270718 disrupts the DNA binding of all four B-ZIP proteins at a concentration in the range of 5–10 μM; however, it does not displace ethidium bromide. In contrast, NSC311152 displaces all four B-ZIP proteins from DNA and also displaces ethidium bromide from DNA at similar concentrations, suggesting that the displacement of B-ZIP proteins from DNA is an indirect effect of binding to DNA. This assay shows that of the 12 active compounds from the fluorescence polarization assay that were tested, 6 displaced ethidium bromide, suggesting that they bind to DNA, and 6 were inactive in this assay, suggesting that they may bind to the B-ZIP protein. Fig. 7 summarizes the data for 12 compounds tested in both assays. (For a description of the physical and chemical properties of the molecules, visit http://129.43.27.140/ncidb2.)

DNA binding assay

EMSA was used as a secondary screen to identify compounds that could inhibit the DNA binding of protein|DNA complexes. We examined all six compounds that were positive in the primary screen and negative in the ethidium bromide screen as well as two compounds that were positive in the ethidium bromide screen (NSC176327 and NSC7223) for the ability to inhibit the DNA binding of five B-ZIP proteins or one B-HLH-ZIP domain protein bound to their cognate site. SREBP-1 is a B-HLH-ZIP protein that is structurally similar to the B-ZIP proteins used in the primary screen [21]. The ability of small molecules to inhibit the DNA binding of B-ZIP and B-HLH-ZIP protein was initially tested by adding 20 μM compound to 20 nM protein bound to radiolabeled DNA. Of the six compounds that were negative in the ethidium displacement assay, two (NSC13778 and NSC146443) were able to inhibit DNA binding. We titrated these two compounds against protein|DNA complexes to examine their activity and specificity of action. NSC13778 showed some specificity in which B-ZIP protein it could inhibit (Fig. 8A); for example, the DNA binding of C/EBPα is abolished at 100 nM, whereas the related protein C/EBPβ took 500 nM. In contrast, NSC146443 showed little specificity, with 200 nM compound being required to inhibit the DNA binding of four proteins and 500 nM being required to inhibit the DNA binding of two proteins (Fig. 8B).

Both compounds that were active in the ethidium bromide displacements assay were also active in the EMSA assay. NSC176327 has some specificity in which protein binding reaction is inhibited. Only 100 nM inhibits the DNA binding of SREBP-1, whereas 500 nM is needed to inhibit the DNA binding of the majority of the other proteins. As an example of a compound that was inactive in the fluorescence polarization assay, NSC328481 did not show any ability to inhibit the DNA binding activity of any protein used in this study, even at 20 μM (Fig. 8D).

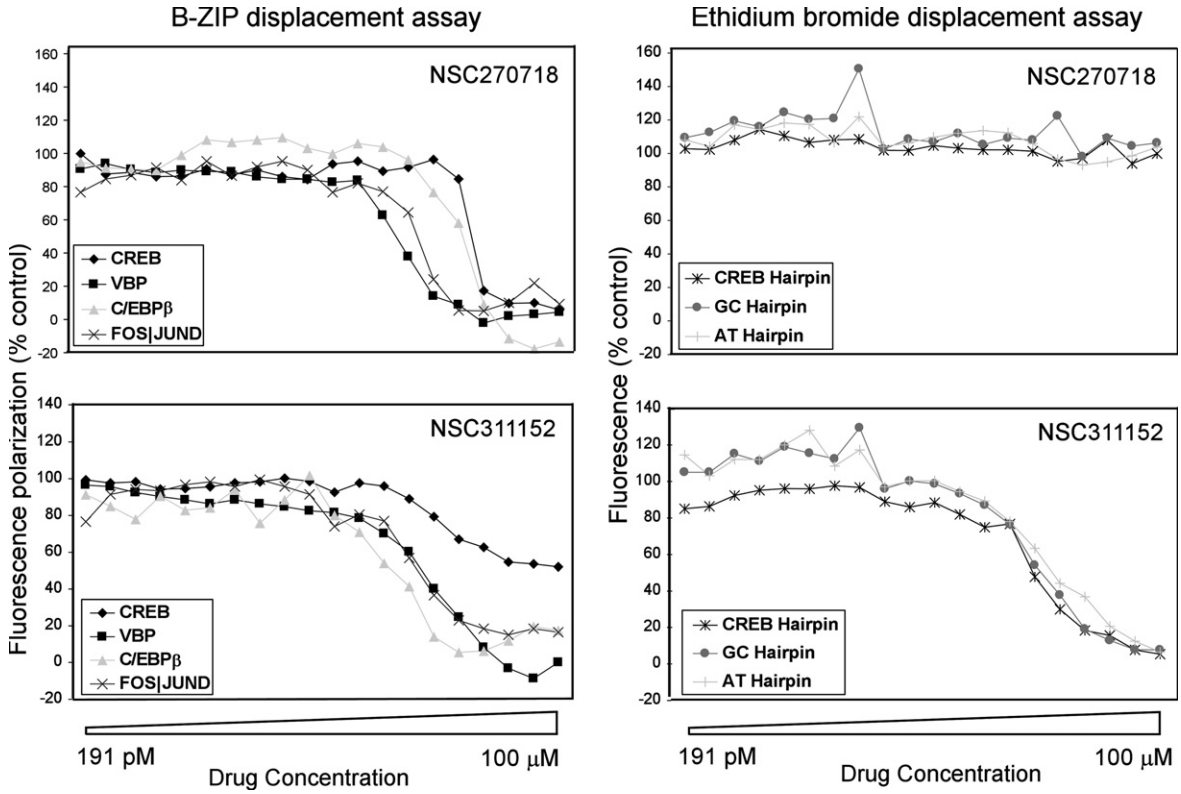

Fig. 6. Identification of compounds that bind to DNA. From the initial screen, 12 actives were tested at 20 dilutions in both the fluorescence polarization B-ZIP binding assay and the ethidium bromide displacement assay. For example, NSC311152 is active in both assays, indicating that the compound is likely binding to the DNA. In contrast, NSC270718 is active only in the fluorescence polarization B-ZIP displacement assay, indicating that the compound may be binding to the protein.

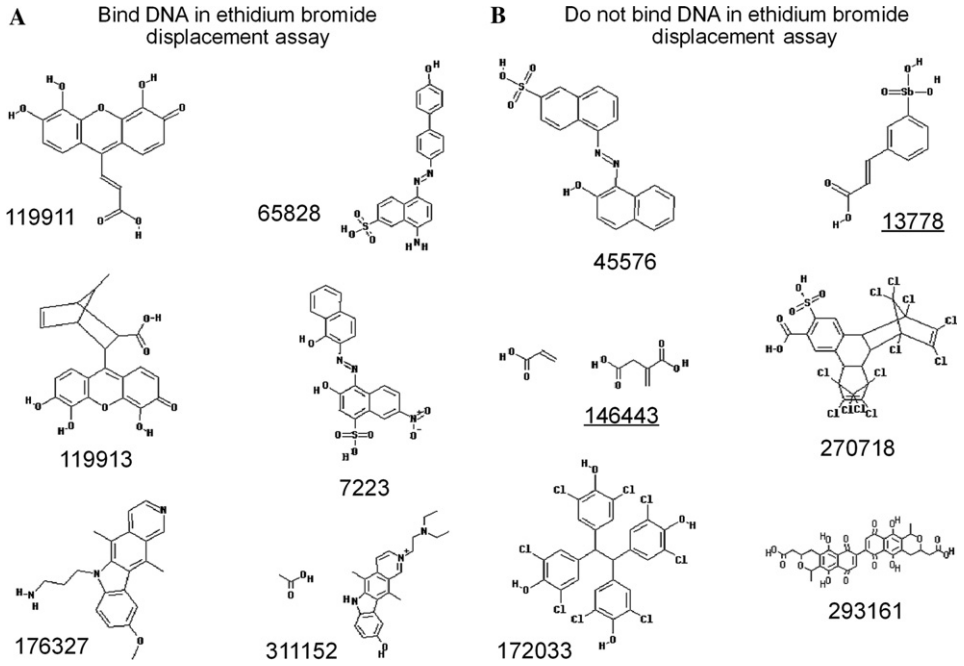

Fig. 7. Structures of 12 compounds tested in both the fluorescence polarization B-ZIP binding assay and the ethidium bromide displacement assay. Underlined compounds bind to the B-ZIP domain in CD thermal denaturation assay.

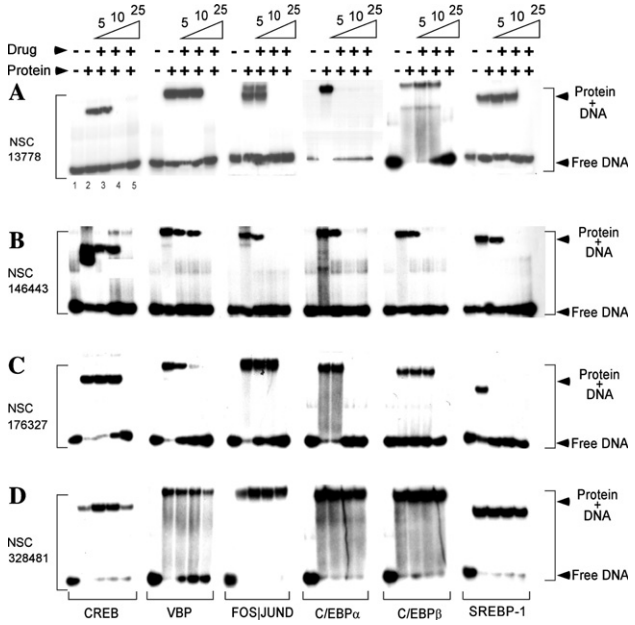

Fig. 8. EMSA examining the inhibition of six protein|DNA complexes by small molecules, showing that 20 nM (dimer) of CREB, VBP, FOS|JUND, C/EBPα, C/EBPβ, and SREBP-1 bound to 7 pg of 28-bp, 5′-end, radiolabeled double-stranded DNA containing their cognate binding site (see text for details): (A) NSC13778; (B) NSC146443; (C) NSC176327; (D) NSC328481. For panels A, B, and D, compound concentration in lane 3 = 100 nM, in lane 4 = 200 nM, and in lane 5 = 500 nM. For the polymer NSC146443, 5, 10, and 25 ng were added to lanes 3, 4, and 5, respectively.

Circular dichroism spectroscopy

We used CD spectroscopy to determine whether these molecules bind the B-ZIP domain, as assayed by a change in the α-helical structure of the B-ZIP domain or its thermal stability. Many of the compounds tested needed to be dissolved in DMSO and were used in both the high-throughput screen and EMSA at a DMSO concentration of 0.1%. However, the presence of DMSO produces a large scatter in the far-UV CD spectra, obscuring the 222-nm signal that is typically used to estimate α-helical content of a protein and monitor the stability as it is thermally denatured. Fig. 9A presents far-UV CD spectra of C/EBPα in the absence and presence of increasing concentrations of DMSO. A DMSO concentration as low as 0.05% totally obscured the optical signal under 217 nm. However, CD signals remain unchanged at 227 nm in DMSO concentrations between 0.05 and 0.2%, enabling us to study the thermal denaturation of proteins at this wavelength. Fig. 9B shows thermal denaturation curves of C/EBPα at 227 nm in the absence and presence of 0.1% DMSO. These curves overlap, validating our efforts to study thermal denaturation under these conditions. Thermodynamic stability parameters obtained when thermal transition curves were fitted according to a nonlinear equation that assumes the transition between dimer and 2 monomer to be of a two-state type [18] were independent of wavelength used (222/227 nm) to monitor denaturation and were not affected by the presence of 0.1% DMSO.

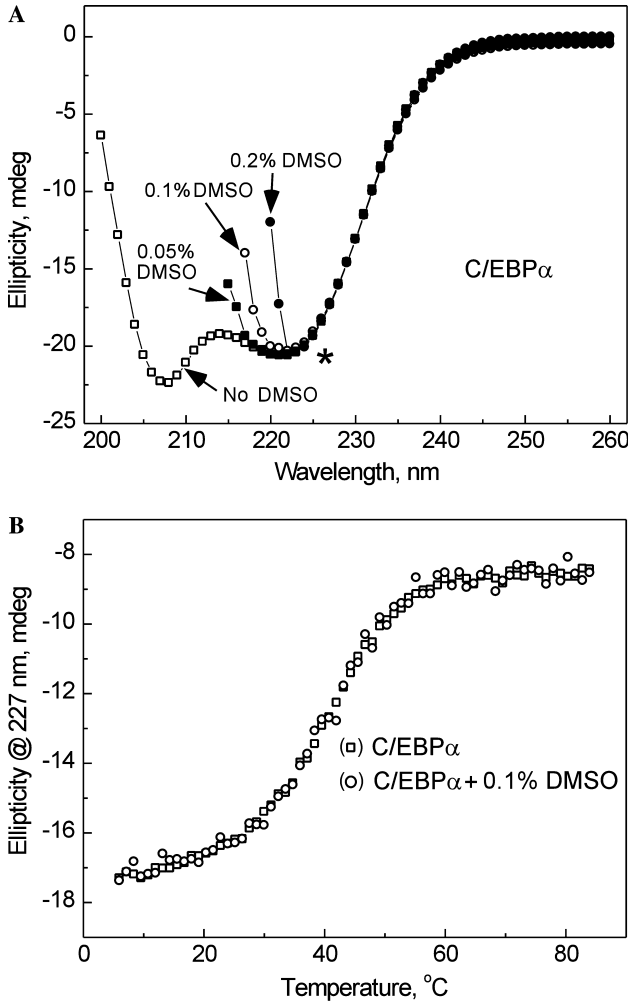

Fig. 9. Effect of DMSO on CD spectrum and thermal stability of C/EBPα. (A) Far-UV CD spectra of 2 μM dimer C/EBPα at 6 °C in the absence and presence of increasing concentrations of DMSO (0.05–0.2%). Asterisk indicates the wavelength (227 nm) at which thermal denaturation of protein was monitored. (B) Thermal stability curves of C/EBPα in the absence and presence of 0.1% DMSO at 227 nm.

The two compounds that were positive in the florescence anisotropy screen and EMSA but negative in the ethidium bromide displacement assay (NSC13778 and NSC146443) were further tested for their ability to bind to the B-ZIP domain using CD spectroscopy. No change in the CD spectrum was observed by the addition of 75 μM NSC13778 to five of the proteins tested by EMSA (FOS|JUND was not tested). However, CD thermal denaturation indicates that NSC13778 binds C/EBPα and stabilizes the protein (Fig. 10A). In addition, 2 μM of the C/EBPα B-ZIP domain dimer is stabilized by 2.8 kcal mol^{-1} $dimer^{-1}$ by 75 μM of NSC13778 (Table 3). This stability arises due to increased melting tem-

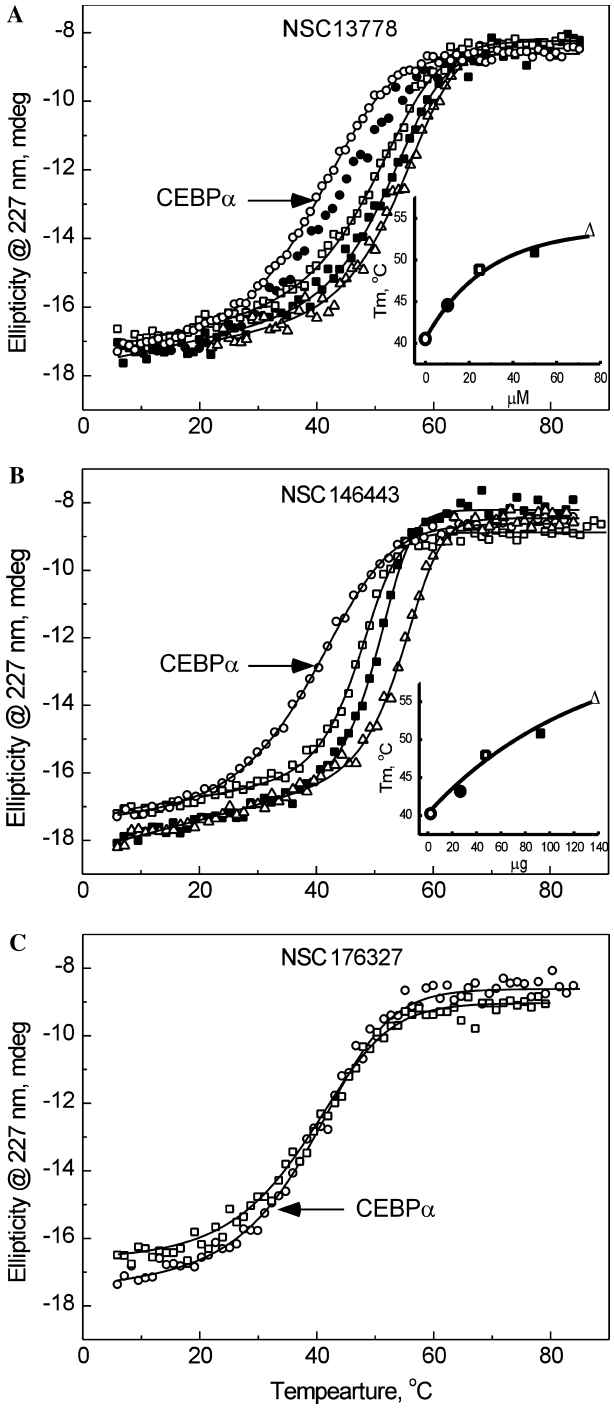

Fig. 10. CD thermal denaturation of C/EBPα in 0.1% DMSO in the presence of small molecules obtained by following changes in CD optical signal at 227 nm. (A) Temperature-induced unfolding of 2 μM dimer C/EBPα in the presence of NSC13778: 0 μM (○), 10 μM (●), 25 μM (□), 50 μM (■), and 75 μM (△). Solid lines through the transition curves are the nonlinear fit, assuming protein denaturations to be two-state. The inset shows the T_m versus NSC13378 concentration. (B) Temperature-induced unfolding of 2 μM dimer (45 μg) C/EBPα in the presence of NSC146443 concentrations: 0 μg (○), 45 μg (□), 90 μg (■), and 135 μg (△). The curve at 25 μg NSC146443 concentration is not shown. The inset shows the T_m versus NSC146443 concentration. (C) Thermal denaturation curve of 2 μM dimer C/EBPα in the absence and presence of 50 μM NSC176327.

perature as well as a favorable enthalpy change on compound binding. The inset in Fig. 10A shows the increasing T_m of C/EBPα with increasing concentrations of NSC13778. Saturation of binding sites seems to occur at 75 μM of NSC13778, with higher concentrations of NSC13778 producing increased noise-to-signal ratios and resulting in an uninterpretable scatter at higher temperatures. CD thermal denaturations with additional B-ZIP proteins and SREBP-1 indicate that NSC13778 also binds these proteins (Table 3), as is expected from the EMSA data.

CD thermal denaturation studies show that C/EBPα domains are stabilized in the presence of NSC146443, as expected from the EMSA data (Table 3). Because this molecule is a polymer, all concentration measurements were in grams of equivalent weight. Increasing concentrations of NSC146443 increased both the T_m and enthalpy change of C/EBPα (Fig. 10B). The inset in Fig. 10B presents the T_m of C/EBPα at different NSC146443 concentrations. The binding seems to be less saturable, at least in the concentration range used in this study, than that observed for NSC13778. We could not study thermal denaturation of C/EBPα at higher NSC146443 concentrations (>135 μg) due to the increase in noise-to-signal ratio, especially at higher temperatures.

The four compounds that were active in florescence anisotropy experiments but negative in both ethidium bromide displacement assay and EMSA (NSC45576, NSC270718, NSC172033, and NSC293161) were also tested using CD spectroscopy. These four compounds, at 50 μM, did not increase the T_m of any of the proteins used in the EMSA (FOS|JUND was not tested). The putative DNA binder NSC176327 that was active in EMSA was also tested in our CD spectroscopy screen. Thermal denaturation was carried out in the absence and presence of 50 μM NSC176327 (Fig. 10C). As expected, there was no change in the thermal stability of C/EBPα in its presence, suggesting that the protein has no binding site for this molecule.

We mapped the binding of NSC13778 to the basic region of the B-ZIP domain using two proteins. NSC13778 did not bind a protein having the basic region replaced with an acidic sequence (A-C/EBPα) [18], suggesting that the binding site is in the basic region (results not shown). Similar results were obtained with 0H-C/EBPα, a protein lacking the DNA binding basic region [18] (results not shown).

A more detailed mapping of the binding of NSC13778 to the basic region of the B-ZIP domain used two similar proteins: C/EBPα and C/EBPβ. At 25 μM, NSC13778 preferentially binds C/EBPα, increasing the T_m by 8 °C. The C/EBPβ B-ZIP domain has a T_m of 65 °C, the highest T_m for any described B-ZIP domain. We presume that C/EBPβ is more stable than C/EBPα due to the glutamic acid instead of aspartic acid in the

Table 3
Thermodynamic parameters associated with thermal denaturation of B-ZIP and B-HLH-ZIP proteins in the presence of small molecules

Protein	[NSC13778] (μM)	T_m (°C)	ΔH_m (kcal mol^{-1} dimer^{-1})[a]	ΔG_{Di} (37 °C) (kcal mol^{-1} dimer^{-1})[b]	[NSC146443] (μg)	T_m (°C)	ΔH_m (kcal mol^{-1} dimer^{-1})	ΔG_{Di} (37 °C) (kcal mol^{-1} dimer^{-1})
C/EBPα	0	40.5	–45 ± 4	–8.6 ± 0.2	0	40.5	–45 ± 4	–8.6 ± 0.2
	10	43.2	–49 ± 2	–9.1 ± 0.1	10	42.9	–53 ± 2	–9.1 ± 0.1
	25	48.7	–46 ± 3	–9.8 ± 0.2	25	47.9	–96 ± 3	–11.4 ± 0.2
	50	50.9	–55 ± 2	–10.5 ± 0.1	90	50.8	–102 ± 4	–12.5 ± 0.2
	75	53.2	–65 ± 3	–11.4 ± 0.2	135	55.3	–96 ± 3	–13.5 ± 0.2
C/EBPβ	0	65.5	–55 ± 5	–12.4 ± 0.4				
C/EBPβ(α)	0	66.5	–69 ± 5	–13.9 ± 0.3				
	25	69.8	–67 ± 3	–14.1 ± 0.2				
C/EBPα(β)	0	44.0	–36 ± 4	–8.5 ± 0.1				
	50	44.5	–29 ± 6	–8.3 ± 0.1				
CREB	0	49.0	–60 ± 2	–10.4 ± 0.4				
	25	49.6	–54 ± 3	–10.3 ± 0.2				
	75	54.5	–61 ± 6	–11.5 ± 0.4				
VBP	0	42.7	–54 ± 2	–9.1 ± 0.1				
	25	42.9	–57 ± 4	–9.1 ± 0.2				
	75	44.2	–60 ± 2	–9.4 ± 0.1				
SREBP-1	0	49.5	–51 ± 3	–10.1 ± 0.1				
	25	51.5	–55 ± 5	–10.6 ± 0.2				
	75	53.3	–57 ± 4	–11.0 ± 0.2				

[a] Each ΔH_m value is the mean of three independent measurements (± standard error).
[b] The error in values of ΔG_{Di} is due to error in ΔH_m and ΔC_p values.

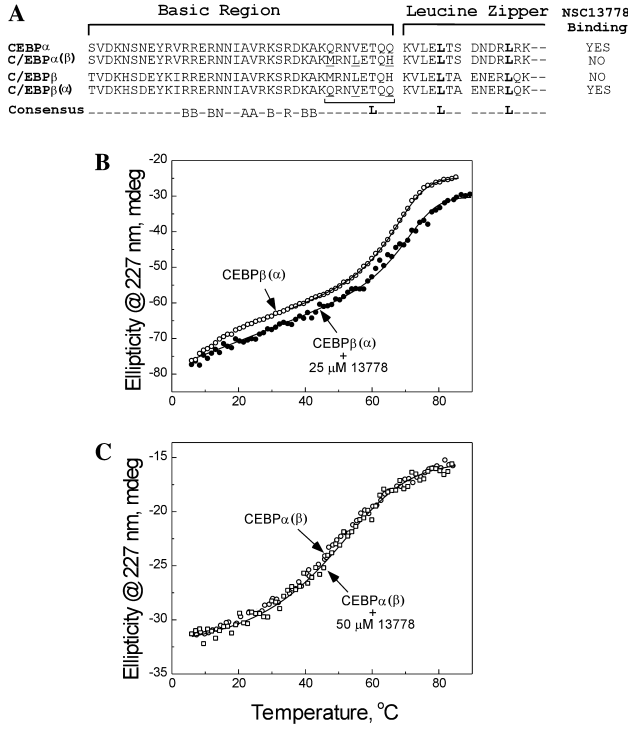

Fig. 11. Binding of NSC13778 to C/EBP chimeric proteins as studied by CD thermal denaturation at 227 nm. (A) Amino acid sequence of the basic region and part of the leucine zipper of C/EBPα and C/EBPβ and their chimeric derivatives, C/EBPα(β) and C/EBPβ(α). Underlined amino acids in C/EBPα(β) are from C/EBPβ, whereas those in C/EBPβ(α) are from C/EBPα. To the right is a summary of whether the protein binds NSC13778. At the bottom is a consensus sequence for B-ZIP proteins. (B) Thermal transition curve of 4 μM dimer C/EBPβ(α) in the absence and presence of 25 μM NSC13778. All solutions were in CD buffer containing 0.1% DMSO. (C) C/EBPα(β) thermal stability with or without 50 μM NSC13778.

g position of the second heptad [26,27]. The DNA binding basic regions of C/EBPα and C/EBPβ differ in seven amino acids: four clustered in the N terminal of the basic region and three clustered at the junction of the basic region and the leucine zipper (Fig. 11A). We produced two chimeric proteins by placing the three amino acids from C/EBPα (Q, V, and Q) at the junction region into C/EBPβ to produce C/EBPβ(α). Likewise, the three amino acids from C/EBPβ (M, L, and H) were placed into C/EBPα to produce C/EBPα(β) (Fig. 11A). These

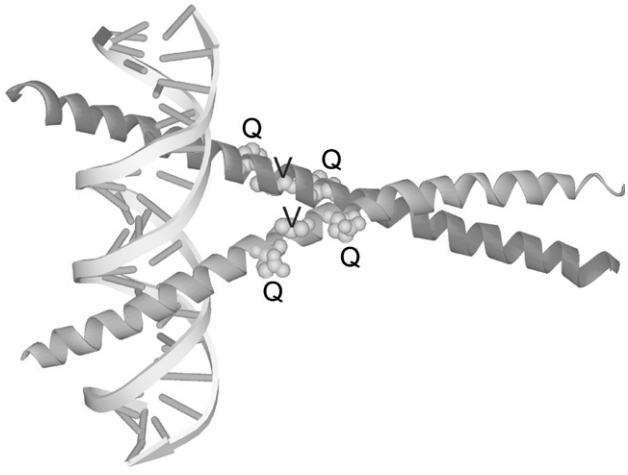

Fig. 12. Co-crystal structure of C/EBPα and 21-bp double-stranded DNA containing C/EBP binding site [28]. The protein and DNA are shown in shades of gray. The positions of amino acids Q, V, and Q in a helical dimer are indicated. The chimeric protein C/EBPα(β) has these three amino acids replaced by M, L, and H. In chimeric C/EBPβ(α), M, L, and H are replaced by Q, V, and Q, respectively.

chimeric proteins had stability similar to that of the parental proteins, indicating that these amino acids do not contribute to protein stability. NSC13778 at 25 μM binds to C/EBPβ(α) but not to C/EBPα(β) (Figs. 11B and C). These data, plus the binding of NSC13778 to C/EBPα but not to C/EBPβ, maps the binding to these three amino acids (Q, V, and Q). Positions of these three amino acids in the helical dimer are highlighted on the crystal structure of C/EBPα [28] (Fig. 12).

Discussion

We have developed a high-throughput fluorescence polarization screen to identify small molecules that disrupt the DNA binding of B-ZIP proteins to DNA. We screened the NCI diversity set of 1990 compounds using four B-ZIP dimers (CREB, C/EBPβ, VBP, and FOS|-JUND) and identified 39 compounds that were active against at least one protein|DNA complex. Confirmation titrations identified 21 compounds that disrupted DNA binding in the micromolar range. We used three secondary screens to evaluate 12 representative compounds identified in the fluorescent polarization screen: (i) an ethidium bromide displacement assay to identify compounds that bind to DNA, (ii) an EMSA to identify compounds that disrupt the protein|DNA complex, and (iii) a CD thermal denaturation assay to identify compounds that bind and stabilize the B-ZIP motif. These assays identified two compounds (NSC13778 and NSC146443) that bound to the basic region of the B-ZIP domain, each with some specificity, and stabilized the protein.

Unlike most protein–protein interactions, where each protein has a well-defined structure in the absence of its partner(s), the basic region of B-ZIP proteins is unstructured in the absence of DNA [29,30]. However, in the presence of DNA, the basic region undergoes a structural transition and becomes α-helical, and the protein is stabilized [23]. Both active molecules, NSC13778 and NSC146443, bind the basic region of the B-ZIP motif. Like DNA, the binding of NSC146443 induces a small increase in new α-helical structure, as may be expected from a negatively charged polymer. NSC13778, in contrast, did not induce any new α-helical structure. NSC13778 is a small molecule (MW 319) that contains an antimony atom. At 500 nM (25× protein), NSC13778 abolished the DNA binding of all the proteins examined, suggesting that it binds to the basic region of the transcription factors. Surprisingly, the EMSA data show the discrimination that this compound displayed for binding C/EBPα and C/EBPβ. CD thermal denaturation experiments with 50 μM NSC13778 indicate that C/EBPα is stabilized by 1.9 kcal mol^{-1} $dimer^{-1}$, whereas C/EBPβ is not. By using mutant chimeric proteins of C/EBP, C/EBPβ(α) and C/EBPα(β), we were able to map the specific region of the basic motif of C/EBPα to which NSC13778 binds. It prefers to bind the three amino acids (Q, V, and Q) that are on the same side of the α-helical basic region of C/EBPα and not M, L, and H from C/EBPβ. It remains to be determined whether these amino acids are in α-helical structure when bound by NSC13778. The absence of charged amino acids in the critical amino acids suggests that the specificity is not primarily electrostatic.

The data presented here indicate that the unstructured basic region of both B-ZIP and B-HLH-ZIP proteins is a potential molecular target for small molecule binding. This is a different type of target from most cases given that the target itself is unstructured and may become structured on binding of the small molecule.

References

[1] L.T. Vassilev, B.T. Vu, B. Graves, D. Carvajal, F. Podlaski, Z. Filipovic, N. Kong, U. Kammlott, C. Lukacs, C. Klein, N. Fotouhi, E.A. Liu, In vivo activation of the p53 pathway by small-molecule antagonists of MDM2, Science 303 (2004) 844–848.

[2] C. Vinson, M. Myakishev, A. Acharya, A.A. Mir, J.R. Moll, M. Bonovich, Classification of human B-ZIP proteins based on dimerization properties, Mol. Cell. Biol. 22 (2002) 6321–6335.

[3] R. Eferl, E.F. Wagner, AP-1: a double-edged sword in tumorigenesis, Nat. Rev. Cancer 3 (2003) 859–868.

[4] M.R. Young, J.J. Li, M. Rincon, R.A. Flavell, B.K. Sathyanarayana, R. Hunziker, N. Colburn, Transgenic mice demonstrate AP-1 (activator protein-1) transactivation is required for tumor promotion, Proc. Natl. Acad. Sci. USA 96 (1999) 9827–9832.

[5] S. Herzig, F. Long, U.S. Jhala, S. Hedrick, R. Quinn, A. Bauer, D. Rudolph, G. Schutz, C. Yoon, P. Puigserver, B. Spiegelman, M. Montminy, CREB regulates hepatic gluconeogenesis through the coactivator PGC-1, Nature 413 (2001) 179–183.

[6] S. Herzig, S. Hedrick, I. Morantte, S.H. Koo, F. Galimi, M. Montminy, CREB controls hepatic lipid metabolism through nuclear hormone receptor PPAR-gamma, Nature 426 (2003) 190–193.

[7] S. Zhu, K. Yoon, E. Sterneck, P.F. Johnson, R.C. Smart, CCAAT/Enhancer binding protein-beta is a mediator of keratinocyte survival and skin tumorigenesis involving oncogenic Ras signaling, Proc. Natl. Acad. Sci. USA 99 (2002) 207–212.

[8] M.S. Nasir, M.E. Jolley, Fluorescence polarization: an analytical tool for immunoassay and drug discovery, Comb. Chem. High Throughput Screen. 2 (1999) 177–190.

[9] V.K. Vinson, E.M. De la Cruz, H.N. Higgs, T.D. Pollard, Interactions of *Acanthamoeba profilin* with actin and nucleotides bound to actin, Biochemistry 37 (1998) 10871–10880.

[10] R. Seethala, R. Menzel, A fluorescence polarization competition immunoassay for tyrosine kinases, Anal. Biochem. 255 (1998) 257–262.

[11] S.Z. Schade, M.E. Jolley, B.J. Sarauer, L.G. Simonson, BODIPY-alpha-casein, a pH-independent protein substrate for protease assays using fluorescence polarization, Anal. Biochem. 243 (1996) 1–7.

[12] P. Banks, M. Gosselin, L. Prystay, Fluorescence polarization assays for high throughput screening of G protein-coupled receptors, J. Biomol. Screen. 5 (2000) 159–168.

[13] P. Wu, M. Brasseur, U. Schindler, A high-throughput STAT binding assay using fluorescence polarization, Anal. Biochem. 249 (1997) 29–36.

[14] R.H. Shoemaker, D.A. Scudiero, G. Melillo, M.J. Currens, A.P. Monks, A.A. Rabow, D.G. Covell, E.A. Sausville, Application of high-throughput, molecular-targeted screening to anticancer drug discovery, Curr. Top. Med. Chem. 2 (2002) 229–246.

[15] C.J. Glover, K. Hite, R. DeLosh, D.A. Scudiero, M.J. Fivash, L.R. Smith, R.J. Fisher, J.W. Wu, Y. Shi, R.A. Kipp, G.L. McLendon, E.A. Sausville, R.H. Shoemaker, A high-throughput screen for identification of molecular mimics of Smac/DIABLO utilizing a fluorescence polarization assay, Anal. Biochem. 320 (2003) 157–169.

[16] A. Rapisarda, B. Uranchimeg, D.A. Scudiero, M. Selby, E.A. Sausville, R.H. Shoemaker, G. Melillo, Identification of small molecule inhibitors of hypoxia-inducible factor 1 transcriptional activation pathway, Cancer Res. 62 (2002) 4316–4324.

[17] J.R. Moll, M. Olive, C. Vinson, Attractive interhelical electrostatic interactions in the proline- and acidic-rich region (PAR) leucine zipper subfamily preclude heterodimerization with other basic leucine zipper subfamilies, J. Biol. Chem. 275 (2000) 34826–34832.

[18] D. Krylov, M. Olive, C. Vinson, Extending dimerization interfaces: the bZIP basic region can form a coiled coil, EMBO J. 14 (1995) 5329–5337.

[19] S. Ahn, M. Olive, S. Aggarwal, D. Krylov, D.D. Ginty, C. Vinson, A dominant–negative inhibitor of CREB reveals that it is a general mediator of stimulus-dependent transcription of c-fos, Mol. Cell. Biol. 18 (1998) 967–977.

[20] M. Olive, D. Krylov, D.R. Echlin, K. Gardner, E. Taparowsky, C. Vinson, A dominant negative to activation protein-1 (AP1) that abolishes DNA binding and inhibits oncogenesis, J. Biol. Chem. 272 (1997) 18586–18594.

[21] V. Rishi, J. Gal, D. Krylov, J. Fridriksson, M.S. Boysen, S. Mandrup, C. Vinson, SREBP-1 dimerization specificity maps to both the HLH and leucine zipper domains: Use of a dominant negative, J. Biol. Chem. 279 (2003) 11863–11874.

[22] D.L. Boger, B.E. Fink, S.R. Brunette, W.C. Tse, M.P. Hedrick, A simple, high-resolution method for establishing DNA binding affinity and sequence selectivity, J. Am. Chem. Soc. 123 (2001) 5878–5891.

[23] J.R. Moll, A. Acharya, J. Gal, A.A. Mir, C. Vinson, Magnesium is required for specific DNA binding of the CREB B-ZIP domain, Nucleic Acids Res. 30 (2002) 1240–1246.

[24] T. Ellenberger, C. Brandl, K. Struhl, S. Harrison, The GCN4 basic region leucine zipper binds DNA as a dimer of uninterrupted α helices: crystal structure of the protein–DNA complex, Cell 71 (1992) 1223–1237.

[25] J.H. Zhang, T.D. Chung, K.R. Oldenburg, A simple statistical parameter for use in evaluation and validation of high throughput screening assays, J. Biomol. Screen. 4 (1999) 67–73.

[26] D. Krylov, I. Mikhailenko, C. Vinson, A thermodynamic scale for leucine zipper stability and dimerization specificity: e and g interhelical interactions, EMBO J. 13 (1994) 2849–2861.

[27] D. Krylov, J. Barchi, C. Vinson, Inter-helical interactions in the leucine zipper coiled coil dimer: pH and salt dependence of coupling energy between charged amino acids, J. Mol. Biol. 279 (1998) 959–972.

[28] M. Miller, J.D. Shuman, T. Sebastian, Z. Dauter, P.F. Johnson, Structural basis for DNA recognition by the basic region leucine zipper transcription factor CCAAT/enhancer-binding protein alpha, J. Biol. Chem. 278 (2003) 15178–15184.

[29] J.D. Shuman, C.R. Vinson, S.L. McKnight, Evidence of changes in protease sensitivity and subunit exchange rate on DNA binding by C/EBP, Science 249 (1990) 771–774.

[30] K.T. O'Neil, J.D. Shuman, C. Ampe, W.F. DeGrado, DNA-induced increase in the alpha-helical content of C/EBP and GCN4, Biochemistry 30 (1991) 9030–9034.